Effect of nematic ordering on the elasticity and yielding in disordered polymeric solids

Andrea Giuntoli[1], Nicola Calonaci[1,a], Sebastiano Bernini[1], Dino Leporini[1,2]

[1]Dipartimento di Fisica "Enrico Fermi", Università di Pisa, Largo B.Pontecorvo 3, I-56127 Pisa, Italy
[2]Istituto per i Processi Chimico-Fisici-Consiglio Nazionale delle Ricerche (IPCF-CNR), via G. Moruzzi 1, I-56124 Pisa, Italy

Correspondence to: D.Leporini (E-mail: dino.leporini@unipi.it)

Dated: November 20, 2018

ABSTRACT The relation between elasticity and yielding is investigated in a model polymer solid by Molecular-Dynamics simulations. By changing the bending stiffness of the chain and the bond length, semicrystalline and disordered glassy polymers - both with bond disorder - as well as nematic glassy polymers with bond ordering are obtained. It is found that in systems with bond disorder the ratio τ_Y/G between the shear yield strength τ_Y and the shear modulus G is close to the universal value of the atomic metallic glasses. The increase of the local nematic order in glasses leads to the increase of the shear modulus and the decrease of the shear yield strength, as observed in experiments on nematic thermosets. A tentative explanation of the subsequent reduction of the ratio τ_Y/G in terms of the distributions of the per-monomer stress is offered.

Keywords: Elasticity, Yield, Polymer Glass, Nematic Glass, Molecular-Dynamics simulation

[a] present address: International School for Advanced Studies (SISSA), via Bonomea 265, 34136 Trieste, Italy

INTRODUCTION

The understanding of the microscopic mechanisms underlying the plastic response of amorphous solids to externally driven deformations is a current issue in material science research both for the lack of a complete theoretical background and its importance in technical applications.[1–4] Solids subjected to small deformations respond linearly as expected from elasticity theories.[5–8] An increasing strain on the system causes the increase of internal stress. Focusing on pure shear deformation, the elastic modulus G of the system under the studied deformation can be derived from the slope of the stress-strain curve in the small strain regime[3] both locally and globally[9]. Upon increasing strain, amorphous solids show complex and far from linear behavior[10–12], with heterogeneous and protocol-dependent[13,14] phenomena taking place mainly due to the absence of long-range order[1]. Having reached a characteristic yield strain, corresponding to the shear yield strength τ_Y, the transition from the (reversible) elastic state to the (irreversible) plastic one takes place[2,15,16]. In an ideal elasto-plastic body (Hooke-St.Venant) τ_Y is the maximum stress[2].

Despite the complexity of the plastic behavior in amorphous solids at the local scale, some general features have been found in the macroscopic quantities. An interesting aspect of yielding is that the yield stress is proportional to the elastic modulus. In particular, for a linear, dislocation-free array of atoms Frenkel derived long time ago the relation $\tau_Y/G \simeq 1/(\pi\sqrt{3}) \simeq 0.18$ at $T = 0K$[2,17,18]. A more recent experimental work found $\tau_Y/G \sim 0.11$ for polymers[1] and the universal value 0.036 ± 0.002 for metallic atomic glasses[19]. The ratio τ_Y/G depends on the temperature and, for a given temperature, is universal for metallic glasses up to slightly below the glass transition temperature[19]. The finding has been interpreted in terms of similar inter-particle potentials[20]. The microscopic origin of the proportionality between τ_Y and G has been rationalized by noting that in both metals and polymers the yield stress is primarily governed by energy storing elastic processes: dislocation line energy in metals, strain energy around molecular kinks in polymers[5]. Since the elastic modulus in glassy polymers is dominated by intermolecular forces[21], it was concluded that the energy barriers to plastic flow in glassy polymers were dominated by intermolecular rather than intra-molecular interactions[1],
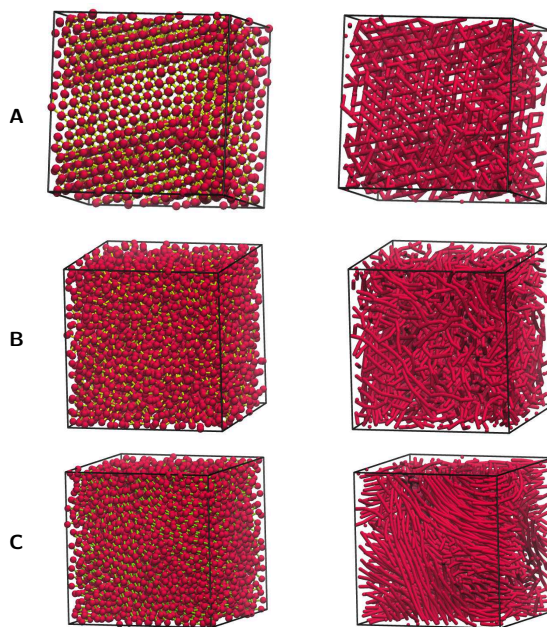

Figure 1: Illustrative snapshots of the different polymer solids under study: semicrystalline polymer (A), disordered glassy polymer (B), nematic glassy polymer (C). Monomer position is emphasized in the left column, bond orientation is emphasized in the right column. Differently from the nematic glassy polymer, both semicrystalline and disordered glassy polymers exhibit local bond disorder. The snapshots refer to chains with bond length $l_b = 1.12$ and bending stiffness $k_\theta = 0$ (A), 4 (B), 12.5 (C).

so some similarities can be found in the comparison between atomic and polymeric systems[22]. On the other hand, the intra-molecular interactions can have a primary role in determining the structure of a polymer solid upon cooling from the liquid phase, which is of great importance to determine the elastic properties of the final structure[13,14].

The aim of this work is to investigate the existence of the correlation of shear elastic modulus G and yielding stress τ_Y in polymer solids by means of molecular dynamics (MD) simulations. A model is presented in which the systematic variation of characteristic parameters of the intra-molecular interactions, namely the bond length l_b and the bending stiffness k_θ of pairs of contiguous bonds

in a chain, leads to different semicrystalline, disordered or nematic structures, see Fig. 1. For fully-flexible chains with no bending potential ($k_\theta = 0$) we find that the yield stress increases with the elastic modulus in a way which is very close to the universal law of the atomic metallic glasses [19], suggesting that, in the absence of bending stiffness, connectivity and structure play minor roles in the yield process of the present polymer model. Increasing the bending stiffness of the chains causes the increasing growth of the local nematic ordering of near chains. It is seen that the onset of nematic order *increases* the elastic modulus G and *decreases* the yielding stress τ_Y, thus evidencing the different influence of the local order on the plasticity and the elasticity. A tentative explanation of the subsequent reduction of the ratio τ_Y/G in terms of the distributions of the per-monomer stress is offered.

NUMERICAL METHODS

We consider a coarse-grained polymer model of $N_c = 160$ linear, unentangled chains with $M = 25$ monomers per chain. The total number of monomers is $N = 4000$. Non-bonded monomers at distance r interact via the truncated and shifted Lennard-Jones (LJ) potential:

$$U^{LJ}(r) = \varepsilon \left[\left(\frac{\sigma^*}{r} \right)^{12} - 2 \left(\frac{\sigma^*}{r} \right)^6 \right] + U_{cut} \quad (1)$$

for $r \leq r_c = 2.5\sigma$ and zero otherwise, where $\sigma^* = 2^{1/6}\sigma$, is the position of the potential minimum with depth ε. The value of the constant U_{cut} is chosen to ensure that $U_{LJ}(r)$ is continuous at $r = r_c$. Henceforth, all quantities are expressed in terms of reduced units: lengths in units of σ, temperatures in units of ε/k_B (with k_B the Boltzmann constant) and time τ_{MD} in units of $\sigma\sqrt{m/\varepsilon}$ where m is the monomer mass. We set $m = k_B = 1$. The bonding interaction is approximated via the harmonic potential

$$U_{bond}(r) = k_b(r - l_b)^2 \quad (2)$$

where l_b is the equilibrium bond length and $k_b = 300\varepsilon/\sigma^2$ is the bond rigidity. Differently from previous studies concerning fully-flexible chains [23–26], the bending angle interaction between adjacent chemical bonds is included through a potential of the form [27]:

$$U_{bending} = k_\theta(1 - \cos\theta_b) \quad (3)$$

where k_θ is the bending stiffness, $\cos\theta_b^i = \vec{b}_{i+1} \cdot \vec{b}_i/||\vec{b}_{i+1}|| ||\vec{b}_i||$ and the bond vector $\vec{b}_i = \vec{r}_{i+1} - \vec{r}_i$, where $\vec{r}_i$ is the position of the i-th monomer. Periodic boundary conditions are used. The study was performed in the NPT ensemble (constant number of particles, pressure and temperature). The integration time step is set to $\Delta t = 0.005$ time units [26,28]. The simulations were carried out using LAMMPS molecular dynamics software (http://lammps.sandia.gov). [29]

A systematic study is performed by changing the bond length l_b and bending stiffness k_θ. We focus on two families of systems: fully flexible polymers ($k_\theta = 0$) with $0.91 \leq l_b \leq 1.12$, and semi-flexible/stiff polymers with $l_b = 1.12$ and $1.0 \leq k_\theta \leq 12.5$. All samples are equilibrated in the NPT ensemble at $P = 0$. They are initially equilibrated at the following temperatures: $T = 1.2$ for $k_\theta < 7$, $T = 1.4$ for $7 \leq k_\theta < 12.5$, $T = 1.6$ for $k_\theta = 12.5$. Then, they are isobarically cooled down to $T = 0$ with a constant quench rate of $|\dot{T}| = 2 \cdot 10^{-6}$. Both the equilibration and the quench procedures are close to the one adopted in Ref. [27]. Isobaric quenches have also been considered in other MD investigations of plastic yield in glassy polymers. [16] After the quench, simple shear deformations of the polymer solids at $T = 0$, $P = 0$ are performed via the Athermal Quasi-Static (AQS) protocol described in details in Ref. [3]. Initially, the undeformed simulation box containing the sample is a cube with side L. An infinitesimal strain increment $\Delta\varepsilon = 10^{-5}L$ is applied, after which the system is allowed to relax in the local potential energy minimum via a suitable minimization algorithm. The procedure is repeated up to the total strain $\varepsilon_{tot} = 15 \cdot 10^{-2}L$.

Simple shear is performed independently in the planes (xy, xz, yz), and at each strain step in the plane $\alpha\beta$ the corresponding component of the macroscopic stress tensor $\tau_{\alpha,\beta}$ is taken as the average value of the per-monomer stress $\tau_{\alpha,\beta}^i$:

$$\tau_{\alpha,\beta} = \frac{1}{N} \sum_{i=1}^{N} \tau_{\alpha,\beta}^i \quad (4)$$

In an athermal system the expression of the per-monomer stress in the atomic representation is [30]:

$$\tau_{\alpha,\beta}^i = \frac{1}{2v} \sum_{j \neq i} r_{\alpha ij} F_{\beta ij} \quad (5)$$

3

where $F_{\gamma kl}$ and $r_{\gamma kl}$ are the γ components of the force between the kth and the lth monomer and their separation, respectively, and v is the average per-monomer volume, i.e. $v = L^3/N$. For each plane we then obtain a stress-strain curve, an illustrative example of which is given in Fig. 2. The result is quite analogous to what reported for many other systems under athermal conditions[31–36] with an initial linear increase followed by increasing bending and onset of the plastic regime. In particular, similarly to other MD studies of glassy polymers[37], one notices that, in the plastic regime, the stress levels off to a plateau with fluctuations caused by subsequent loading phases and sudden stress drops. We point out that the initial non-zero stress in the unstrained solid seen in Fig. 2 is a well-known phenomenon usually ascribed to the limited size of the simulation cell[38].

We measure the shear elastic modulus G as the slope of the stress-strain curve in the linear regime ($\varepsilon \leq 0.01$), via the relation $G = \tau/2\varepsilon$, see inset of Fig. 2. Following Ref.[20], the yield stress τ_Y is taken as the average value of the stress after the first significant plastic event, defined as the first stress drop of at least $\Delta\tau_{th} = 0.1$, see Fig. 2. This choice is consistent with other definitions in the presence[16], or not[15], of strain softening, i.e. the reduction in stress following yield. The results are robust with respect to changes of $\Delta\tau_{th}$. Data concerning 16 distinct simulation runs are gathered for each physical state. Each run is averaged over the three planes xy, xz and yz.

RESULTS AND DISCUSSION

Structural analysis during quench-cooling

The elastic properties of amorphous solids strongly depend on the sample preparation[13,14]. Thus, we preliminarily characterize the most relevant structural changes of our systems occurring during the isobaric quench from the liquid to the athermal solid.

In order to study more rigorously the structural order of the systems, we resort to the order parameters defined by Steinhardt *et al.*[39]. One considers in a given coordinate system the polar and azimuthal angles $\theta(\mathbf{r}_{ij})$ and $\phi(\mathbf{r}_{ij})$ of the vector $\mathbf{r}_{ij}$ joining the i-th central monomer with the j-th one belonging to the neighbors within a preset cutoff distance $r_{cut} = 1.2 \; \sigma^* \simeq 1.35$[39]. r_{cut} is a convenient definition of the first coordination shell size[40]. The vec-
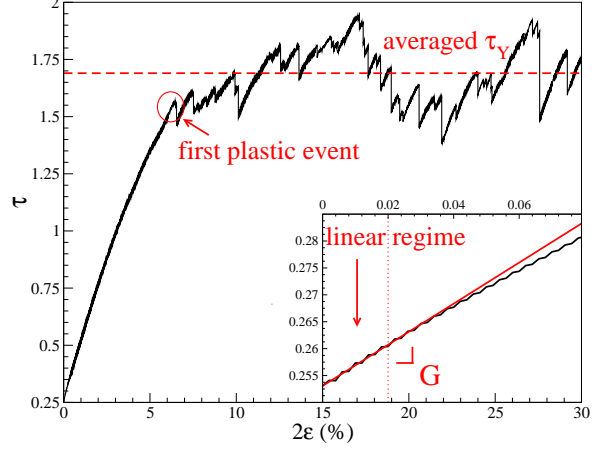

Figure 2: Typical stress-strain curve of our polymer solids under athermal, quasi-static, simple-shear deformation. After a first 'loading' phase, a plateau-like plastic regime sets in where a series of sudden stress drops are observed. The yield stress τ_Y is defined as the average value of τ in the plastic regime[20]. The elastic modulus G (see inset) is measured via a linear fit of the stress-strain curve in the linear regime of small deformations $2\epsilon < 0.02$. The plot refers to a system of fully-flexible chains ($k_\theta = 0$) with bond length $l_b = 1.12$.

tor $\mathbf{r}_{ij}$ is usually referred to as a "bond" and has not to be confused with the *actual* chemical bonds of the polymeric chain. To define a global measure of the order in the system, one then introduces the quantity:

$$\bar{Q}_{lm}^{glob} = \frac{1}{N_b} \sum_{i=1}^{N} \sum_{j=1}^{n_b(i)} Y_{lm}\left[\theta(\mathbf{r}_{ij}), \phi(\mathbf{r}_{ij})\right] \qquad (6)$$

where $n_b(i)$ is the number of bonds of i-th particle, N is the total number of particles in the system, Y_{lm} denotes a spherical harmonic and N_b is the total number of bonds:

$$N_b = \sum_{i=1}^{N} n_b(i) \qquad (7)$$

The global orientational order parameter Q_l^{glob} is defined by[39]:

$$Q_l^{glob} = \left[\frac{4\pi}{(2l+1)} \sum_{m=-l}^{l} |\bar{Q}_{lm}^{glob}|^2 \right]^{1/2} \qquad (8)$$

4

The above quantity is invariant under rotations of the co-ordinate system and takes characteristic values which can be used to quantify the kind and the degree of rotational symmetry in the system[39]. In the absence of *large*-scale order, the bond orientation is uniformly distributed around the unit sphere and Q_l^{glob} is rather small since it vanishes as $\sim N_b^{-1/2}$[41]. On the other hand, Q_6^{glob} is very sensitive to any kind of crystallization and increases significantly when order appears[42,43]. A local orientational parameter Q_l^{loc} can also be defined. We define the auxiliary quantity

$$\bar{Q}_{lm}^{loc}(i) = \frac{1}{n_b(i)} \sum_{j=1}^{n_b(i)} Y_{lm} \left[\theta(\mathbf{r}_{ij}), \phi(\mathbf{r}_{ij}) \right] \qquad (9)$$

The local order parameter Q_l^{loc} is defined as[39]:

$$Q_l^{loc} = \frac{1}{N} \sum_{i=1}^{N} \left[\frac{4\pi}{(2l+1)} \sum_{m=-l}^{l} |\bar{Q}_{lm}^{loc}(i)|^2 \right]^{1/2} \qquad (10)$$

In general $Q_l^{loc} \geq Q_l^{glob}$. In the presence of ideal order, *all* the particles have the *same* neighborhood configuration, and the equality $Q_l^{loc} = Q_l^{glob}$ follows.

We first examine the density and the global order of fully-flexible chains ($k_\theta = 0$). The global positional order of the monomers is monitored via the Steinhardt order parameter Q_6^{glob}. Fig. 3 plots the increase of both the density ρ and the order parameter Q_6^{glob} for different bond lengths l_b while decreasing the temperature at constant pressure $P = 0$ from the initial liquid state to the final solid state. Fully flexible polymers either exhibit global order or glassify upon cooling, depending on the bond length l_b. Global order is revealed by sharp jumps in density ρ and Q_6^{glob} for $l_b = 1.06, 1.09, 1.12$. A local-order analysis, presented later in the paper, clarifies that the states with global order are semicrystalline polymers with coexisting polymorphs at $T = 0$. Systems with shorter bond length form glassy polymers, with no significant global order. If the bond length is comparable to the monomer size, $l_b \approx \sigma^* \simeq 1.12$, the formation of ordered structures is to be expected[43–47], whereas shorter bonds are known[44,48–50] to cause geometrical frustration which hinders the crystallization process, thus favoring the formation of disordered glassy polymers.

We now turn to semi-flexible and stiff chains ($k_\theta > 0$). Since the reduced flexibility favors local nematic order-
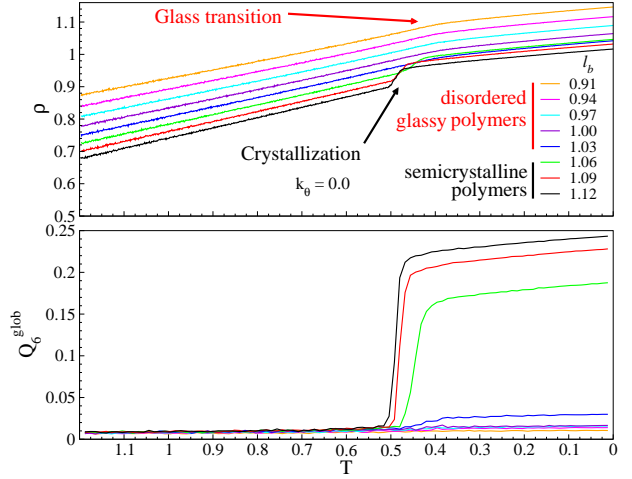

Figure 3: Density ρ (upper panel) and global order parameter Q_6^{glob} (lower panel) of a melt of fully-flexible chains ($k_\theta = 0$) with different bond length l_b during the isobaric quench from the liquid to the solid phase. Chains with short bond length ($l_b \leq 1.03$) form disordered glassy polymers since the bond length is incommensurate with the Lennard-Jones length scale $\sigma^* \simeq 1.12$. Chains with bond length comparable to $\sigma^* \simeq 1.12$ exhibit steep increase of the density ρ and the global order parameter Q_6^{glob} upon cooling. In the latter case, the local-order analysis presented in Fig.6 clarifies that the corresponding solids at $T = 0$ are semicrystalline polymers with coexisting polymorphs.

ing, i.e. the alignment of near bonds, we divide the sample in n^3 cells with side L/n and define the bond-orientation order parameter in the i-th cell as[51]

$$S_i = \sqrt{\frac{3}{2} Tr(q_i^2)}, \quad q_{i,\alpha\beta} = \langle \hat{b}_\alpha \hat{b}_\beta - \frac{1}{3}\delta_{\alpha\beta} \rangle_i \qquad (11)$$

where $1 \leq i \leq n^3$, Tr is the trace operator, q_i is a 3×3 orientational tensor with components of $q_{i,\alpha\beta}$, $\hat{b}_\alpha$ and $\hat{b}_\beta$ are the Cartesian components of the normalized bond vectors $\vec{b}$ and the statistical average $\langle ... \rangle_i$ is performed on all the bonds of the i-th cell. Following Karayiannis and coworkers[27], we initially choose $n = 6$ corresponding to cells with side of about $2 - 3$ monomer diameters. An average local bond-orientation order parameter is then defined as[51]

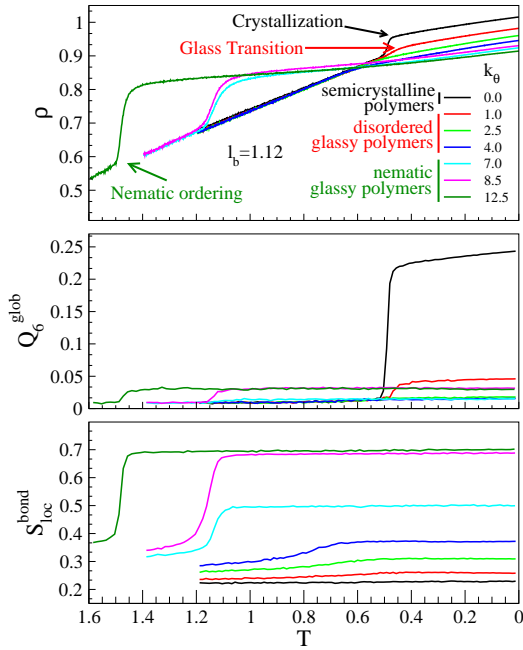$$S_{loc}^{bond} = \frac{1}{216} \sum_{i=1}^{216} S_i \qquad (12)$$

5

Figure 4: Density ρ (top), global order parameter Q_6^{glob} (middle) and local bond-orientation order parameter S_{loc}^{bond} (bottom) of a melt of chains with increasing bending stiffness during the isobaric quench from the liquid to the solid phase. Bond length $l_b = 1.12$. For fully-flexible chains ($k_\theta = 0$) a steep increase of the density ρ and the global order parameter Q_6^{glob} is revealed at $T \simeq 0.5$. For semi rigid/stiff chains ($k_\theta > 0$): i) all the final solid states are glassy polymers ($Q_6^{glob} < 0.05$), ii) on cooling, the bending stiffness triggers a transition to a nematic state with bond ordering occurring in the liquid phase and freezing below the glass transition.

The S_{loc}^{bond} order parameter ranges between $S_{loc}^{bond} = 1$ (perfect alignment) and $S_{loc}^{bond} = 0$ (random orientation). Fig. 4 plots the density ρ, the order parameter Q_6^{glob} and the local bond-orientation order parameter S_{loc}^{bond} of systems with bond length $l_b = 1.12$ and different bending stiffness k_θ, during the isobaric quench from the initial liquid state to the final solid state. The latter exhibits global order only if the chains are fully flexible ($k_\theta = 0$), as signaled by the jumps of both the density and the global order parameter at $T \simeq 0.5$, otherwise glassy polymers with small global order ($Q_6^{glob} < 0.05$) are obtained. It
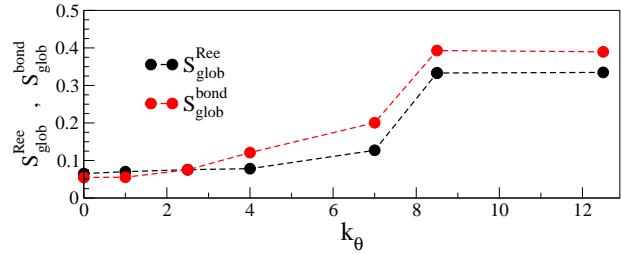

Figure 5: Dependence of the global bond-orientation order parameter S_{glob}^{bond} and the global chain-orientation order parameter S_{glob}^{Ree} on the bending stiffness by increasing k_θ at $T = 0$. Bond length $l_b = 1.12$. Note that, even for high bending stiffness, the global order is not strong despite the local ordering shown in Fig.4 (bottom). See Fig.1 for selected snapshots.

is seen that the increasing bending stiffness of the chains triggers a transition to a nematic state with considerable local alignment of the bonds, as detected by the increase of the bond-orientational order parameter S_{loc}^{bond}. The resulting local orientational order freezes below the glass transition, yielding a nematic glassy polymer.

It is interesting to consider the global bond-orientation order. To this aim, we set $n = 1$ and define the global bond-orientation order parameter S_{glob}^{bond} as S_1 from eq.11 to perform the average of the bond orientation over a *single* cell coinciding with all the sample. The quantity is plotted in Fig.5. On increasing the bending stiffness k_θ at $T = 0$, S_{glob}^{bond} starts from ~ 0.05 for fully-flexible chains ($k_\theta = 0$), then increases and levels off at the plateau level $S_{glob}^{bond} \simeq 0.38$ for $k_\theta \gtrsim 8.5$. This suggests that the sample is *locally oriented* (high S_{loc}^{bond}), but *macroscopically nearly isotropic* (small S_{glob}^{bond}) for strong bending stiffness. To corroborate the previous conclusion, we consider the alignment of the end-to-end unit vector of the chains via the global chain-orientation order parameter S_{glob}^{Ree}[27]. By construction, S_{glob}^{Ree} spans the range between $S_{glob}^{Ree} = 1$ (perfect alignment of all the chains) and $S_{glob}^{Ree} = 0$ (random orientation). Fig.5 shows that S_{glob}^{Ree} increases with the bending stiffness but it is not large.

In order to gain more insight into the structure of the polymeric solids Fig.6 presents the correlation plots of the local order parameters Q_4^{loc} and Q_6^{loc}, characterizing the order of the *first* neighbor shell of each monomer. Fig.6a
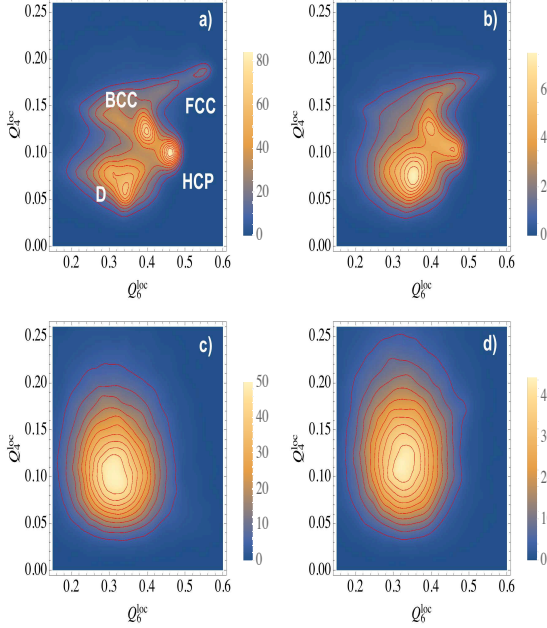
Figure 6: Bivariate distributions of the local order parameters Q_4^{loc} and Q_6^{loc} for characteristic states at $T = 0$: (a) semicrystalline polymer with $l_b = 1.12$ and $k_\theta = 0$; (b) semicrystalline polymer with $l_b = 1.06$ and $k_\theta = 0$; (c) disordered glassy polymer with $l_b = 1.12$ and $k_\theta = 4$; (d) nematic glassy polymer with $l_b = 1.12$ and $k_\theta = 12.5$. In panel a) the regions corresponding to the BCC, FCC and HCP structures at the level of the first neighbor shell are marked. The region "D" labels states with first neighbor shell different from the BCC, FCC and HCP ones. The contour lines have equal contour interval and divide the whole elevation range evenly.

shows the complex nature of the solid state with $l_b = 1.12$ and $k_\theta = 0$, corresponding to fully-flexible chains with bond length comparable to the monomer size. Four different regions with highly-correlated pairs (Q_4^{loc}, Q_6^{loc}) are apparent. According to previous studies[43,52], two of them signal face-centered cubic (FCC) and hexagonal close packed (HCP) local packings. For the same polymer model with $k_\theta = 0$ and $l_b = 1.12$ at $T = 0$, FCC and HCP close packed structures together with other (unspecified) non close-packed environments were detected[27]. We also identify high correlations in the region $(Q_4^{loc}, Q_6^{loc}) \simeq (0.12, 0.4)$. These values are as-

cribed to a deformed body-centered cubic (BCC) structure with (Q_4^{loc}, Q_6^{loc}) pair significantly different from the ideal BCC due to poor stability of the BCC lattice[43,53]. On the basis of previous studies[54], we believe that such BCC structures were nucleated as metastable regions during the quench and frozen in the solid phase at $T = 0$. BCC structures have been reported for the present model with $k_\theta = 0$ and $l_b \simeq 0.97$ in the crystallization of a polymer melt exposed to well-ordered walls[44] and in the spontaneous isothermal crystallization of an unbounded polymer melt[43]. The D region in Fig.6a represents environments with first neighbor shell different from the BCC, FCC and HCP ones.

In summary, the solid state of fully-flexible chains with bond length comparable to the monomer size, $l_b = 1.12 \approx \sigma^*$, is semicrystalline with coexisting polymorphs. The structure of the solid appears to be much less heterogeneous by decreasing the bond length or increasing the bending stiffness. In fact, Fig.6b shows that, if $l_b = 1.06$ with $k_\theta = 0$, the D region is enhanced to the detriment of the BCC, FCC and HCP regions. For $l_b \leq 1.03$ and $k_\theta = 0$ the solid is a disordered glass and only the D region is apparent (not shown). A similar finding is observed by keeping $l_b = 1.12$ and increasing the strength of the bending potential, see c) and d) panels of Fig.6. Then, we see that the D region is characteristic of our glassy systems.

We note that Fig.6d shows two weak lobes located at $Q_6^{loc} \simeq 0.48$ with $Q_4^{loc} \simeq 0.09$ and 0.175. By comparison with panels a) and c) of Fig.6, the finding suggests reentrant FCC and HCP ordering on increasing the strength of the bending potential with $l_b = 1.12$. The finding is consistent with the results reported by Karayiannis and coworkers[27] where the fraction of sites with close-packed order (FCC or HCP similarities) is close to one in systems with $S_{glob}^{Ree} \simeq 1$, i.e. nearly straight chains, and high local orientation order, $S_{loc}^{bond} \sim 0.95$. We remind that in our case S_{glob}^{Ree} and S_{loc}^{bond} are not larger than about 0.33 and 0.7, respectively. Incidentally, the fact that we find less global and local orientational order with the same polymer model with respect to Ref.[27] is ascribed to the smaller size of our sample.
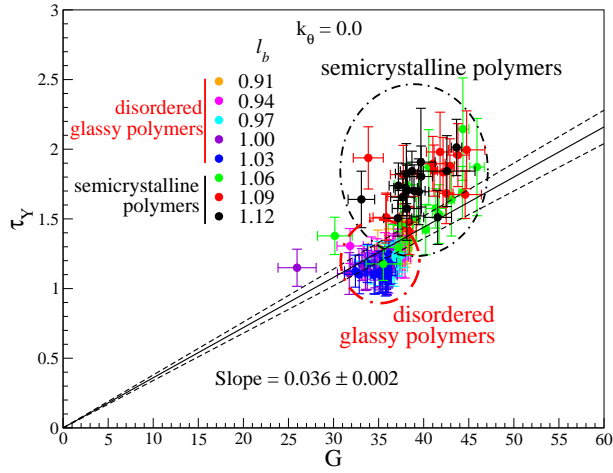
Figure 7: Correlation plot of the elastic modulus G and the average yield stress τ_Y for the athermal solids made by fully-flexible chains with different bond lengths. The error bars of τ_Y and G reflect the fluctuation of the stress during the steady state of the plastic regime, and the uncertainty of the fit in the linear elastic regime, see Fig. 2, respectively. Semicrystalline polymers and disordered glassy polymers exhibit correlations in two different regions, inside of which the influence of the bond length is minor. The black continuous line is the universal law of metallic glasses $\tau_Y = m\,G$ with slope $m = 0.036 \pm 0.002$[19]. The uncertainty on the m parameter is bounded by the two dashed lines.

Correlation between yield stress and shear modulus

Fig. 7 is a correlation plot of the average yield stress τ_Y and the elastic shear modulus G for the solids made by fully-flexible chains with different bond lengths l_b. The plot presents the data on a run-by-run basis, i.e. no average between runs with the same bond length is performed. A general tendency of the yield stress τ_Y to increase with the modulus is observed. It is seen that disordered glassy polymers exhibit limited changes of both τ_Y and G, whereas semicrystalline polymers show a wider distribution across the different runs. We ascribe the effect to the polymorphic character of the ordered solids[43]. Also, semicrystalline polymers show higher G and τ_Y values with respect to disordered glassy polymers, meaning that the increased order of the monomeric arrangement causes
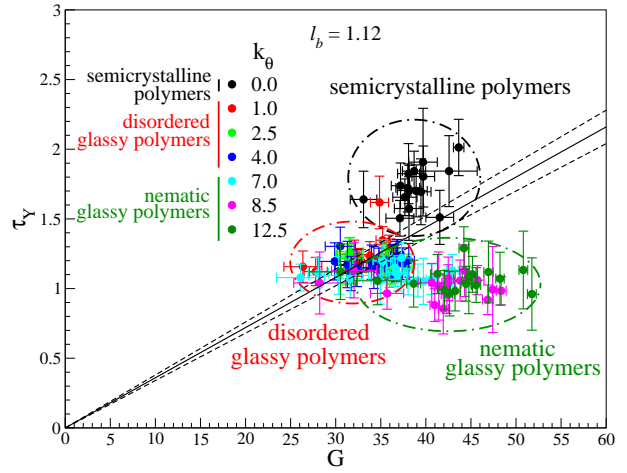
Figure 8: Correlation plot of the elastic modulus G and the average yield stress τ_Y for the athermal solids made by chains with different bending stiffness. Bond length $l_b = 1.12$. As in Fig. 7 the black continuous line is the universal law of metallic glasses $\tau_Y = m\,G$ with slope $m = 0.036 \pm 0.002$[19]. Differently from semicrystalline and disordered glassy polymers, *nematic glassy polymers* exhibit large deviations from that law.

the system to react to shear deformations with stronger internal stresses with respect to its amorphous counterpart both in the linear regime and at the yield point. In Fig. 7 we superimpose to our data the characteristic universal law of the metallic *atomic* glasses, i.e. the line $\tau_Y = m\,G$ with $m = 0.036 \pm 0.002$[19]. Deviations are apparent but not large, thus suggesting that, in the absence of bending stiffness, connectivity and structure play minor roles in the yield process of the present polymer model.

The introduction of bending stiffness, $k_\theta \neq 0$, and the subsequent nematic order provide a different scenario. This is clearly visible in the correlation plot of the average yield stress τ_Y and the elastic shear modulus G, see Fig. 8. For low and intermediate bending stiffness, $k_\theta \leq 4$, the solids are semicrystalline polymers or microscopically disordered glassy polymers respectively, with ratio τ_Y / G close to the characteristic universal value 0.036 ± 0.002 of the atomic metallic glasses[19], as in Fig. 7. For nematic glassy polymers, $k_\theta \geq 7$, the ratio τ_Y / G decreases by increasing the bending stiffness of the chain.
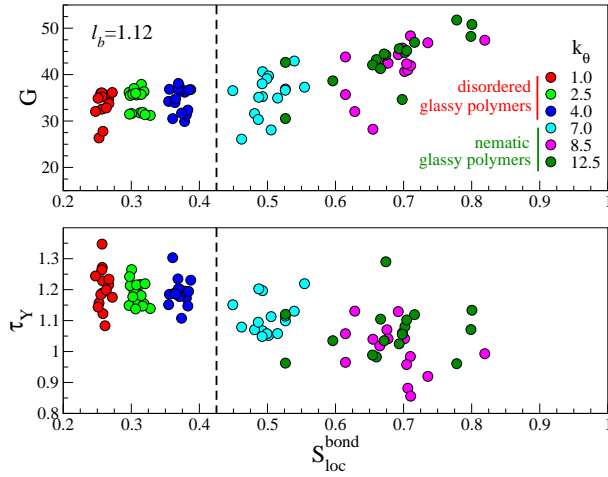
We have investigated the origin of the deviations of the

Figure 9: Correlation between the elastic modulus (top) and the yield stress τ_Y (bottom) with the local bond-orientation order parameter S_{loc}^{bond}, Eq.12. Bond length $l_b = 1.12$. The dashed line divides the regions pertaining to disordered (left) and nematic (right) glassy polymers. It is seen that in nematic glassy polymers the increasing local bond alignment *increases* the elastic modulus and *decreases* the yield stress.

Figure 10: Correlation between the elastic modulus (top) and the yield stress τ_Y (bottom) with the density. Bond length $l_b = 1.12$. The dashed line divides the regions pertaining to disordered (left) and nematic (right) glassy polymers. Notice that the nematic glassy polymers with $k_\theta = 7$ and $k_\theta = 8.5$ have nearly identical densities but rather different local nematic order, see Fig. 4 top. The fact that their modulus and yield stress are appreciably different signals the influence of the bond ordering.

ratio τ_Y / G from the characteristic universal value of the atomic metallic glasses. Elasticity and yielding of polymeric solids are both affected by density[2] and local nematic order[55–57], two properties which are changed by varying the bending stiffness, see Fig. 4. We first consider the influence of nematic order. Fig. 9 shows that in nematic glassy polymers, on increasing the local orientational order of the bonds, the elastic modulus *increases* and the yield stress *decreases*. A similar effect has been observed by Ortiz et al[57] in the glassy phase of a macroscopically disordered, liquid-crystalline thermoset, where changing the densely cross-linked network structure from an ensemble of randomly oriented rigid-rods to local nematic increases the modulus and decreases the yield stress, see Table 3 and 4 of Ref.[57]. Since the increase of the nematic order is accompanied by the decrease of the density (apart from a small inversion on increasing k_θ from 7 to 8.5, see Fig. 4 top), we have also examined the role of the density. Fig. 10 shows that in disordered glassy polymers, in spite of a density change of about 6% neither
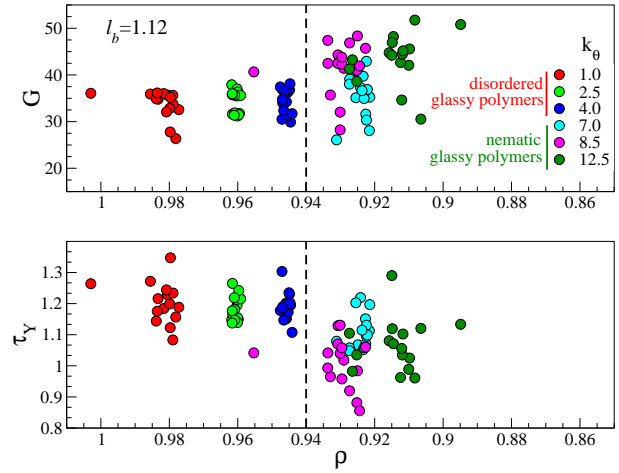
G nor τ_Y change appreciably. Changes are visible in nematic glassy polymers where density changes are smaller due to the better packing. This suggests that density plays a minor role, with respect to nematic order, in setting both the modulus and the yield stress. In this regard, the comparison between the nematic glassy polymers with bending stiffness $k_\theta = 7$ and $k_\theta = 8.5$ provides more insight. The two systems have rather comparable density but quite different local nematic order, see Fig. 4. Fig. 10 shows that their moduli (yield stress) are distinctly different, increasing (decreasing) with the local nematic order. All in all, the discussion of Fig. 9 and Fig. 10 points to the conclusion that in the polymer model under study elasticity and yielding are more affected by the local nematic order than packing. The weak role of packing was also noted in other studies concerning the fast dynamics of polymers[58].

Finally, Fig. 11 plots the per-monomer shear stress distributions in semicrystalline polymers ($k_\theta = 0$), disordered ($k_\theta = 4.0$) and nematic ($k_\theta = 12.5$) glassy poly-

mers. It is seen that the nematic glassy polymer exhibit the broadest distribution with heavy non-gaussian tails. This finding suggests a tentative explanation of the reduction of the ratio τ_Y/G in nematic glassy polymers with respect to semicrystalline polymers and disordered glassy polymers, see Fig. 8. In fact, it is known that application of a local stress τ' decreases the energy barrier ΔE for plastic rearrangements to $\Delta E - \tau' V^\star$ where $V^\star$ is an activation volume [2,5]. If the energy barrier is due to the elastic resistance of the surroundings treated as an isotropic continuum, one finds $\Delta E = GV^\dagger$, where $V^\dagger$ is a further activation volume distinct from $V^\star$ [1,2,59,60]. If one assumes that yielding at $T = 0K$ occurs when the energy barrier vanishes, one finds that the local yield stress $\tau'_Y = V^\dagger/V^\star G$. If the stress distribution is narrow, the local stresses little differ from the average stress, $\tau_Y \simeq \tau'_Y = V^\dagger/V^\star G$, and one recovers the usual coupling between the elastic modulus and the macroscopic yield stress. Otherwise, if the distribution broadens, highly stressed regions yield when the average stress is much less than their stress τ', so that $\tau_Y < V^\dagger/V^\star G$, namely the ratio τ_Y/G decreases with respect to the characteristic value for systems with narrow stress distribution. We are aware that our arguments are rather rough. Nonetheless, they offer a consistent picture leading to the scenario of Fig. 8.
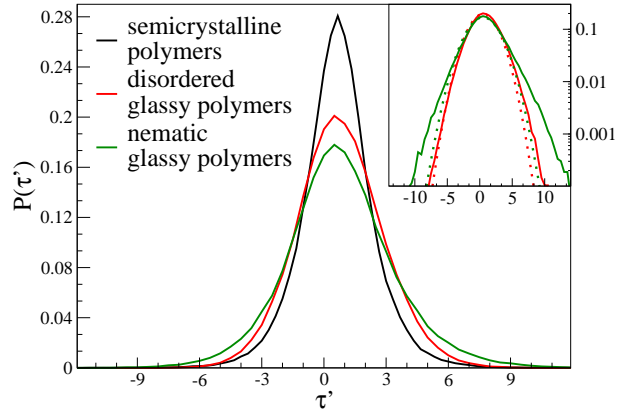

Figure 11: Distribution of the per-monomer shear stress, Eq.5, in semicrystalline polymers ($k_\theta = 0$), disordered ($k_\theta = 4.0$) and nematic ($k_\theta = 12.5$) glassy polymers. All systems have bond length $l_b = 1.12$ and subjected to average stress $\tau = 0.5$, exceeding the linear elastic regime but still far from the region where the sharp plastic drops are observed, see Fig. 2. Inset: comparison between the distributions of the disordered and the nematic glassy polymers. The dotted curves are the best-fit with gaussians showing that the distribution of the nematic glassy polymer exhibits heavy non-gaussian tails.

CONCLUSIONS

Elasticity and yielding in polymer solids have been investigated by MD simulations of a coarse-grained model of linear chains with different bending stiffness and bond length. Following the isobaric quench at $T = 0$, three kind of distinct structures are observed:

- disordered glassy polymers: systems with no positional order and and no bond-orientational order,

- nematic glassy polymers: systems with no local positional order but a strong degree of local bond ordering,

- semicrystalline polymers: systems with local positional order and no bond-orientational order.

Note that in this model system semicrystalline polymers do not have any bond orientational order but in other models, e.g. the CG-PVA model [61], short chains with $M \le 30$ form unfolded semicrystalline structures with both local positional (2D hexagonal) and local bond-orientational order [62,63].

Under simple shear deformations, it is found that in systems with bond disorder the ratio τ_Y/G between the shear yield strength τ_Y and the shear modulus G is close to the universal value of the atomic metallic glasses. In the presence of increasing nematic ordering the shear modulus of the glassy polymer increases while the shear yield strength decreases, thus reducing the ratio τ_Y/G. The finding parallels similar experimental results concerning nematic thermosets. The results suggest that nematic order has stronger influence than density on elasticity and yielding. A tentative explanation of the reduction of the ratio τ_Y/G in nematic glassy polymers with respect to semicrystalline polymers and disordered glassy polymers is offered, pointing out the larger width of the per-monomer stress distributions.

References

1. Argon, A. S. *The Physics of Deformation and Fracture of Polymers*; Cambridge University Press, 2013.

2. Stachurski, Z. H. *Progr. Polymer Sci.* **1997**, *22*, 407–474.

3. Barrat, J. L.; Lemaitre, A. Heterogeneities in amorphous systems under shear. In *Dynamical heterogeneities in glasses, colloids, and granular media*; Berthier, L., Biroli, G., Bouchaud, J., Cipelletti, L., van Saarloos, W., Eds.; Oxford university press, 2011; Chapter 8, pp 264–297.

4. Kramer, E. J. *J. Polymer Sci. Part B: Polymer Phys.* **2005**, *43*, 3369–3371.

5. Argon, A. S. *Phil. Mag.* **1973**, *28*, 839–865.

6. Eshelby, J. D. *Proc. Roy. Soc. London* **1957**, *A241*, 376–396.

7. Budiansky, B. *Phys. Solids* **1965**, *13*, 223–227.

8. Ward, I. M. *Structure and Properties of Oriented Polymers*; J. Wiley & Sons, New York, 1975.

9. Mizuno, H.; Mossa, S.; Barrat, J.-L. *Phys. Rev. E* **2013**, *87*, 042306.

10. Tanguy, A.; Wittmer, J. P.; Leonforte, F.; Barrat, J.-L. *Phys. Rev. B* **2002**, *66*, 174205.

11. Tsamados, M.; Tanguy, A.; Goldenberg, C.; Barrat, J.-L. *Phys. Rev. B* **2004**, *70*, 014203.

12. Tsamados, M.; Tanguy, A.; Goldenberg, C.; Barrat, J.-L. *Phys. Rev. B* **2005**, *72*, 224206.

13. Gendelman, O.; Jaiswal, P. K.; Procaccia, I.; Gupta, B. S.; Zylberg, J. *Europhys. Lett.* **2015**, *109*, 16002.

14. Ashwin, J.; Bouchbinder, E.; Procaccia, I. *Phys. Rev. E* **2013**, *87*, 042310.

15. Hoy, R. S.; Robbins, M. O. *J. Polym. Sci. Part B: Polym. Phys.* **2006**, *44*, 3487–3500.

16. Liu, A. Y.-H.; Rottler, J. *Soft Matter* **2010**, *6*, 4858–4862.

17. Frenkel, J. *Z. Phys.* **1926**, *37*, 572–609.

18. M.G.Northolt,; den Decker, P.; S.J.Picken,; J.J.M.Baltussen,; Schlatmann, R. *Adv. Polym. Sci.* **2005**, *178*, 1–108.

19. Johnson, W. L.; Samwer, K. *Phys. Rev. Lett.* **2005**, *95*, 195501.

20. Lerner, E.; Procaccia, I.; Ching, E. S. C.; Hentschel, H. G. E. *Phys. Rev. B* **2009**, *79*, 180203.

21. Bernini, S.; Leporini, D. *J.Pol.Sci., Part B: Polym. Phys.* **2015**, *53*, 1401–1407.

22. Argon, A. S.; Demkowicz, M. J. *Metall. Mater. Trans.* **2008**, *39A*, 1762–1778.

23. De Michele, C.; Del Gado, E.; Leporini, D. *Soft Matter* **2011**, *7*, 4025–4031.

24. Puosi, F.; Leporini, D. *J. Chem. Phys.* **2012**, *136*, 164901.

25. Puosi, F.; Leporini, D. *J. Chem. Phys.* **2013**, *139*, 029901.

26. Puosi, F.; Leporini, D. *J.Phys. Chem. B* **2011**, *115*, 14046–14051.

27. Nguyen, H. T.; Smith, T. B.; Hoy, R. S.; Karayiannis, N. C. *J. Chem. Phys.* **2015**, *143*, 144901.

28. Ottochian, A.; Leporini, D. *Philosophical Magazine* **2011**, *91*, 1786–1795.

29. Plimpton, S. *J. Comput. Phys.* **1995**, *117*, 1–19.

30. Allen, M. *Mol. Phys.* **1984**, *52*, 705–716.

31. Mott, P. H.; Argon, A. S.; Suter, U. W. *Philos. Mag. A* **1993**, *67*, 931–978.

32. Falk, M. L.; Langer, J. S. *Phys. Rev. E* **1998**, *57*, 7192.

33. Maeda, K.; Takeuchi, S. *Phys. Stat. Sol.* **1978**, *49*, 685–696.

34. Malandro, D. L.; Lacks, D. J. *J. Chem. Phys.* **1999**, *110*, 4593–4600.

35. Maloney, C.; Lemaitre, A. *Phys. Rev. Lett.* **2004**, *93*, 0160001.

36. Dubey, A. K.; Procaccia, I.; Shor, C. A. B. Z.; Singh, M. *Phys. Rev. Lett.* **2016**, *116*, 085502.

37. Vu-Bac, N.; Bessa, M. A.; Rabczuk, T.; Liu, W. K. *Macromolecules* **2015**, *48*, 6713–6723.

38. Crist, B. In *The Physics of Glassy Polymers, II Ed.*; Haward, R. N., Young, R., Eds.; Springer Science+Business Media, Dordrecht, 1997; Chapter 4, pp 155–212.

39. Steinhardt, P. J.; Nelson, D. R.; Ronchetti, M. *Phys. Rev. B* **1983**, *28*, 784–805.

40. Baschnagel, J.; Varnik, F. *J. Phys.: Condens. Matter* **2005**, *17*, R851–R953.

41. Rintoul, M. D.; Torquato, S. *J. Chem. Phys.* **1996**, *105*, 9258–9265.

42. Richard, P.; Oger, L.; Troadec, J.; Gervois, A. *Phys. Rev. E* **1999**, *60*, 4551.

43. Giuntoli, A.; Bernini, S.; Leporini, D. *J. Non-Cryst. Sol.* **2016**, *453*, 88–93.

44. Mackura, M. E.; Simmons, D. S. *J. Polym. Sci. Part B: Polym. Phys.* **2014**, *52*, 134–140.

45. Karayiannis, N. C.; Foteinopoulou, K.; Laso, M. *J. Chem. Phys.* **2009**, *130*, 074704.

46. Karayiannis, N. C.; Foteinopoulou, K.; Laso, M. *Phys. Rev. Lett.* **2009**, *103*, 045703.

47. Karayiannis, N. C.; Foteinopoulou, K.; Abrams, C. F.; Laso, M. *Soft Matter* **2010**, *6*, 2160–2173.

48. Hamley, I. W. *Introduction to Soft Matter: Synthetic and Biological Self-Assembling Materials, Revised Edition*; John Wiley & Sons, Chichester, 2007.

49. Doye, J. P. K.; Louis, A. A.; Lin, I.-C.; Allen, L. R.; Noya, E. G.; Wilber, A. W.; Kok, H. C.; Lyus, R. *Phys. Chem. Chem. Phys.* **2007**, *9*, 2197–2205.

50. Milstein, F. *Phys. Rev. B* **1970**, *2*, 512–518.

51. Luo, C.; Sommer, J.-U. *Macromolecules* **2011**, *44*, 1523–1529.

52. Bernini, S.; Puosi, F.; Barucco, M.; Leporini, D. *J. Chem. Phys.* **2013**, *139*, 184501.

53. Misra, R. D. *Mathematical Proceedings of the Cambridge Philosophical Society* **1940**, *36*, 173–182.

54. ten Wolde, P. R.; RuizMontero, M. J.; Frenkel, D. *The Journal of Chemical Physics* **1996**, *104*, 9932–9947.

55. Douglas, E. P. Liquid Crystalline Thermosets. In *Encyclopedia of Polymer Science and Technology*; Wiley, New York, 2002; Vol. 3, pp 139–159.

56. Benicewicz, B. C.; Smith, M. E.; Earls, J. D.; Ralph D. Priester, J.; Setz, S. M.; Duran, R. S.; Douglas, E. P. *Macromolecules* **1998**, *31*, 4730–4738.

57. Ortiz, C.; Kim, R.; Rodighiero, E.; Ober, C. K.; Kramer, E. J. *Macromolecules* **1998**, *31*, 4074–4088.

58. Barbieri, A.; Gorini, G.; Leporini, D. *Phys. Rev. E* **2004**, *69*, 061509.

59. Frenkel, J. *Kinetic Theory of Liquids*; Dover Publications, New York, 1955.

60. Li, J. C. M.; Gilman, J. J. *J. Appl. Phys.* **1970**, *41*, 4248–4256.

61. Reith, D.; Meyer, H.; Müller-Plathe, F. *Macromolecules* **2001**, *34*, 2335–2345.

62. Meyer, H.; Müller-Plathe, F. *The Journal of Chemical Physics* **2001**, *115*, 7807–7810.

63. Meyer, H.; Müller-Plathe, F. *Macromolecules* **2002**, *35*, 1241–1252.